Fluid Dynamics & Materials Processing
DOI:10.32604/fdmp.2020.010352
Article

Numerical Evaluation of Residual Water Content after Freezing during the Lyophilization of Platelets

Shaozhi Zhang, Ruoyi Xie, Mengjie Xu and Guangming Chen*

Key Laboratory of Refrigeration and Cryogenic Technology of Zhejiang Province, Institute of Refrigeration and Cryogenics, Zhejiang University, Hangzhou, 310027, China
*Corresponding Author: Guangming Chen. Email: enezsz@zju.edu.cn
Received: 28 February 2020; Accepted: 12 October 2020

Abstract: Pre-freezing is an important stage in freeze-drying processes. For the lyophilization of a cell, freezing not only plays a role for primary dehydration, but it also determines the amount of residual (intracellular or extracellular) water, which in turn can influence the solution properties and the choice of operation parameters. The freezing of human platelets in lyoprotectant solution is theoretically investigated here. A two-parameter model and an Arrhenius expression are used to describe cell membrane permeability and its temperature dependency. It is assumed that the intracellular solution is composed of four components: sodium chloride, trehalose, serum protein and water, while the extracellular solution consists of three components. Non-ideal solution behaviors are predicted using measured data. The concentration of maximally freeze-concentrated solution is estimated on the basis of an assumption of solute hydration. The impacts of lyoprotectant composition and extracellular sub-cooling on intracellular super-cooling and residual water content in the cell are analyzed. The values of activation energy of hydraulic permeability at low temperatures are tested to study their impact on the critical cooling rate. As the mass fraction extracellular lyoprotectant (trehalose+bovineserum albumin) increases from 5 wt% to 20 wt%, the intracellular water content at the end of freezing does not change, but the intracellular solution undergoes much higher super-cooling degree. Increasing the mass ratio of trehalose to bovine serum albumin does not change the intracellular water content, but can mitigate intracellular super-cooling. While 0.05 mol/kg trehalose is loaded into platelet, the total quantity of residual water at the end of freezing may raise by 4.93%. The inclusion of dimethyl sulfoxide (Me_2SO) in protectant may bring negative impacts to the drying stage by increasing the residual water content and lowering the drying temperature.

Keywords: Lyophilization; human platelets; freezing; numerical simulation

Nomenclature

English letters

a_i: the amount of water that solute i could hydrate, g water/g solute
A: surface area of cell membrane, m^2

B: cooling velocity, K/s
B_e: second order Virial coefficient for electrolyte
B_i, B_j: second order Virial coefficient for nonelectrolyte
c_0^{ME}: volume fraction of Me_2SO at the initial state
C_i: third order Virial coefficient for nonelectrolyte
k_{diss}: dissociation coefficient
L_p: hydraulic conductivity, m^2s/kg
m: solute molality, osmol/kg
M: molar mass, kg/mol
N: mole quantity, mol
E_{aL}: activation energy of L_p, J/mol
E_{aP}: activation energy of P_s, J/mol
P_s: permeability of cell membrane to permeable solute, m/s
R: universal gas constant, $J/(mol \cdot K)$
$R_1^{'}$: mass ratio of nonelectrolyte to electrolyte
$R_2^{'}$: mass ratio of trehalose to bovine serum albumin
t: time, s
T: temperature, K
T_f: freezing point, K
T_{ref}: reference temperature, K
$T_m^{'}$: temperature of the maximally concentrated point, K
$T_g^{'}$: glass transition temperature corresponding to maximal concentration, K
υ: partial molar volume, m^3/mol
V_w: intracellular water volume, m^3
W: mass fraction, wt%
$W_g^{'}$: mass fraction of solute in maximally freeze-concentrated solution
x: mole fraction, mol%

Greek letters

ΔT_s: supercooling degree, K
ΔT_{se}: supercooling degree of extracellular solution at the moment of ice nucleation
ΔT_{si}: supercooling degree of intracellular solution
ρ_w: water density, kg/m^3
μ: chemical potential, J/mol
π: osmolality, osmol/kg

Subscripts

e: electrolyte
eq: equilibrium
i: nonelectrolyte i
iso: isotonic
s: soluble solute
w: water
0: initial state

Superscripts

ex: extracellular
in: intracellular

Abbreviations

BSA: bovine serum albumin
IIF: intracellular ice formation
IAC: intracellular water content
Me_2SO: dimethyl sulfoxide

1 Introduction

Freeze-drying is a good way for preservation foods, pharmaceuticals and biomaterials such as microorganism, decellularized tissues. The long-term storage of mammalian cells is usually realized with cryopreservation. Many protocols have been developed with respect to the type and development stage of cell [1]. If mammalian cells can be successfully freeze dried, people worldwide will benefit a lot in many aspects. During recent years, great advances have been achieved with inspiration from the nature [2,3]. Red blood cells, platelets, stem cells, and spermatozoa were freeze dried. The recovery rate and viability level of rehydrated cells differed from one research to another [4–9]. Efforts have also been made to address specific problems involved [10,11]. Some practical or clinical applications of freeze-dried products have been put forward [12,13]. Up to now, no common protocol has been established for lyophilization of human erythrocyte or platelet. Therefore, there are still many researches to be carried out, including those relevant with heat and mass transfer. It is well known that heat and mass transfer studies have played an important role in cryopreservation of biomaterials and freeze-drying of foods and pharmaceuticals. For example, Nakagawa et al. [14] developed a multi-dimensional model in which localized variances of microstructural parameters could be input manually to predict the sublimation kinetics, and verified the model with experiments. Rasetto et al. [15] used a dual-scale model which coupled a three-dimensional model, describing the fluid dynamics in the chamber, and a mono/bi-dimensional model, describing the drying of the product in a vial, to gain knowledge about process dynamics and to improve the performance of the control system. Benson et al. [16] modelled the cryoprotectant transport together with toxicity cost function and numerically solved the optimal control problem, using human oocytes as representative cell type. Cui et al. [17] established a model framework for cryopreservation of one-dimensional artificial tissues and obtained the cell transient and final states during cryopreservation within the whole tissue. These studies about heat and mass transfer phenomena usually afford information about local water content, but not on a microscale. For the freeze-drying of mammalian cells, intracellular water content (IAC) should be distinguished from local water content because of the mass transfer resistance of membrane. In order to preserve the freeze-dried product long, IAC should certainly be controlled. Thus, how IAC changes during the lyophilization process is an interesting and important subject. Currently few targeted researches have been reported about this. Zhao et al. [18] proposed a novel differential scanning calorimetry method to determine trapped water of human red cell after freezing. This method will be difficult for human platelets due to their activation characteristics. Thus, this paper will present a mathematical model to describe the freezing stage of human platelets during freeze-drying so that IAC at the end of freezing stage can be known. Before freezing, the platelets are loaded with trehalose, and the lyoprotectants used are bovine serum albumin (BSA), trehalose and Me_2SO [11,19].

2 Mathematical Model

Some traditional assumptions are made in the establishment of the model: (1) The system keeps isobaric during the freezing stage; (2) No temperature difference exists between intra- and extra- cellular space; (3) The intracellular and extracellular solutions are spatially homogeneous; (4) The ratio of intracellular volume to extracellular volume is very small, thus the efflux of intracellular water has no impact on the composition of extracellular solution; (5) The extracellular solution always keeps thermodynamic

equilibrium with ice at the same temperature; (6) The partial molar volume of water in the solution is equal to the molar volume of pure water; (7) The surface area of cell membrane keeps constant; (8) The heat released can be immediately dissipated. These assumptions were often employed in modeling freezing process of cell or tissue [16–18,20].

The basic parameters of human platelets at physiological state are estimated from the measurements of Armitage [21]. They are listed as follows: volume $V_{iso} = 8.45 \times 10^{-18}$ m^3, intracellular water volume $V_{w0} = 6.56 \times 10^{-18}$ m^3, impermeable volume $V_b = 1.89 \times 10^{-18}$ m^3, surface area $A = 25.46 \times 10^{-12}$ m^2, osmolality $\pi_{iso}^{in} = 0.310$ osmol/kg. All intracellular water is accessible to solute [22]. The intracellular solution is assumed to contain three kinds of solute: NaCl, trehalose and bovine serum albumin, with their mole fraction 77.18/20.75/2.07 reflecting the actual osmolality [23].

The intracellular and extracellular solutions are regarded as non-ideal solutions. A multi-solute osmotic Virial equation that considers the dissociation of one electrolyte is employed to calculate the osmolality [24].

$$\pi = (k_{diss} m_e) + B_e (k_{diss} m_e)^2 + \sum m_i + \sum \left(B_i m_i^2\right) + \sum \left(C_i m_i^3\right) + \left\{ \sum \left[(B_e + B_i) k_{diss} m_e m_i \right] + \sum_{i \neq j} \left[\left(B_i + B_j\right) m_i m_j \right] \right\} \quad (1)$$

where the 3rd order interaction coefficients between solutes have been omitted. The virial coefficients are listed in Tab. 1, where R is mass ratio of solute (trehalose, BSA or Me_2SO) to NaCl [25].

Table 1: Parameters of osmotic Virial equation

Symbol	Meaning/unit	Value or empirical expression	Range
k_{diss}	dissociation coefficient	1.657	
B_N	2nd coefficient of NaCl, kg/mol	0.0467	
B_T	2nd coefficient of trehalose, kg/mol	$0.0731 + 0.00472 \times R + 0.3236 \times 0.2032^R$	$0.452 \leq R \leq 20$
C_T	3rd coefficient of trehalose, (kg/mol)^2	$-0.01573 - 0.2963 \times \exp(-R/1.9449)$	
B_B	2nd coefficient of BSA, kg/mol	$\frac{1957 + 2.518 \times 10^4 \times \exp(-R/2.664) + 9.883 \times 10^5 \times \exp(-R/0.3561)}{1 + 1921/R}$	$0.497 \leq R \leq 18.448$
C_B, (kg/mol)^2	3rd coefficient of BSA	$1.141 \times 10^5 + 7.346 \times 10^6 \times \exp(-R/0.7204)$	
B_N	2nd coefficient of Me_2SO, kg/mol	0.108	$0.5 \leq R \leq 19$

The relationship between the solution osmolality and its freezing point is described by Corti et al. [26]:

$$\pi = -\left(g_1 + g_2 \cdot T_f + g_3 \cdot T_f^2 + g_4 \cdot T_f^3 + g_5/T + g_6 \cdot \ln(T)\right) \times 10^3 \quad 223.15\text{K} \leq T \leq 273.15\text{K} \quad (2)$$

$$\pi = -T/(1.86 + 0.0068\ T) \quad T < 223.15\text{K} \quad (3)$$

where $g_1 = 437.503355$ mol/g, $g_2 = 0.649510272$ mol/g/K, $g_3 = -9.54654944 \times 10^{-4}$mol/g/$K^2$, $g_4 = 6.9108635 \times 10^{-7}$ mol/g/K^3, $g_5 = -5184.155$ mol · K/g, $g_6 = -96.04145$ mol/g .

When the extracellular solution begins to freeze, the cell will lose water due to osmotic difference across the membrane. The change of cell water volume is as follows [27]:

$$dV_w/dT = L_p ART\rho_w\left(\pi^{in} - \pi^{ex}\right)/B \tag{4}$$

For permeable solute, its quantity in the cell is described by:

$$dN_s^{in}/dt = P_s A\rho_w\left(m_s^{ex} - m_s^{in}\right) \tag{5}$$

The hydraulic conductivity L_p and the permeability of cell membrane to solute P_s are functions of temperature:

$$L_p = L_{ref}\exp\left[-\frac{E_{aL}}{R}\left(\frac{1}{T} - \frac{1}{T_{ref}}\right)\right] \tag{7}$$

$$P_s = P_{ref}\exp\left[-\frac{E_{aP}}{R}\left(\frac{1}{T} - \frac{1}{T_{ref}}\right)\right] \tag{8}$$

where $T_{ref} = 295.15$ K, $L_{ref} = 3.960 \times 10^{-14}$ m^{2}s/kg, $E_{aL} = 62.787$ kJ/mol, $P_{ref} = 3.167 \times 10^{-7}$ m/s, $E_{aP} = 49.818$ kJ/mol are obtained from literature [28]. It should be noted that these parameters are based on experimental data above 0°C. Their extrapolations to subzero temperature need to be careful.

The cell volume consists of three parts:

$$V_{cell} = V_w + V_b + V_s \tag{9}$$

where V_b is the nonpermeable volume, V_s is the solute volume.

As the temperature decreases and the cell dehydrates, the intracellular solution may encounter three kinds of route as shown in Fig. 1: (1) Route I, when the ratio B/L_p is low, the intracellular solution will dehydrate to the maximum extent; (2) Route II, when the ratio B/L_p is medium, the intracellular solution will dehydrate, but not to the maximum extent, and change into glass; (3) Route III, when B/L_p is high, intracellular ice will format. To follow the last route, the following conditions should be satisfied: (1) The temperature drops below ice nucleation temperature 238.15 K [29]; (2) Freezable water exists in the cell; (3) The supercooling degree of intracellular solution is larger than supercooling tolerance, 1 K [30].

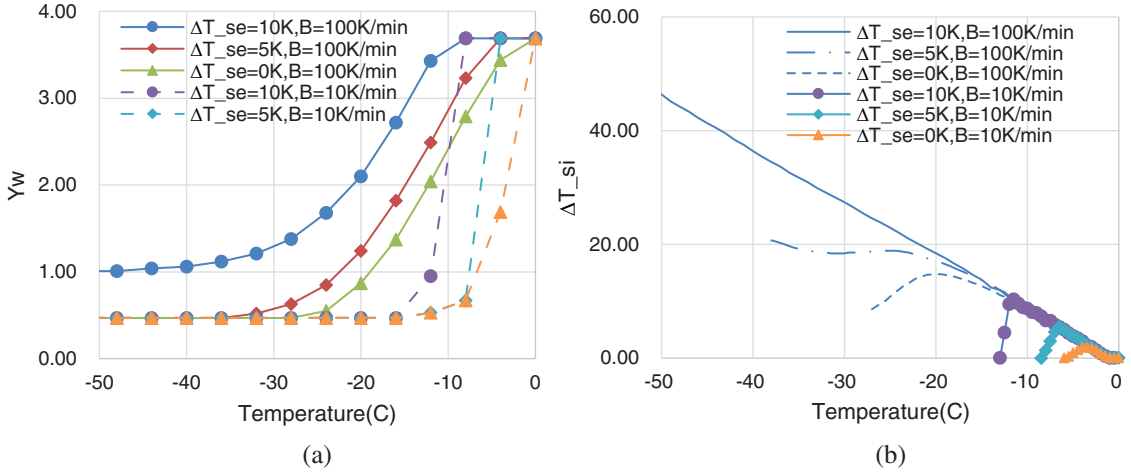

Figure 1: The effects of supercooling degree of extracellular solution ΔT_{se} at the moment of ice nucleation on intracellular water retention ratio Y_w and supercooling degree of intracellular solution ΔT_{si}. (a) Y_w *vs.* temperature at different ΔT_{se} and B, (b) ΔT_{si} *vs.* temperature at different ΔT_{se} and B

With the assumption that each mole of solute hydrated a certain amount of water that cannot be frozen, the concentration of maximally freeze-concentrated solutions $W_g^{'}$ estimated through [31]:

$$W_g^{'} = \sum(W_{i0}) / \sum[(1 + a_i) \cdot W_{i0}] \tag{10}$$

where a_i is the amount of water that solute i could hydrate so that it could not be frozen, W_{i0} is the initial mass fraction of solute i. For NaCl, trehalose, BSA and Me_2SO involved here, their a_i are 1.0671, 0.3135, 0.3891 and 0.4286 g water/g solute respectively.

For a multicomponent solution containing electrolytes, a "modified" Couchman-Karasz (C-K) equation is used to calculate its glass transition temperature T_g:

$$T_g = \frac{\sum\left(\frac{W_i \cdot T_{gi}}{k_i}\right)\left(\frac{\sum W_e}{\sum W_i} + 1\right) + T_{gw}(1 - \sum W_i - \sum W_e)}{\sum\left(\frac{W_i}{k_i}\right)\left(\frac{\sum W_e}{\sum W_i} + 1\right) + (1 - \sum W_i - \sum W_e)} \tag{11}$$

where W_e is the mass fraction of electrolyte; W_i is the mass fraction of nonelectrolyte i; k_i is the C-K coefficient for nonelectrolyte i; T_{gw} is the glass transition temperature of water; T_{gi} is the glass transition temperature of nonelectrolyte i.

The simulation is carried out for a constant-rate cooling process from 293.15 K to 223.15 K. The effects of intracellular lyoprotectant (trehalose and Me_2SO), extracellular lyoprotectant (trehalose, BSA and Me_2SO), supercooling degree of extracellular solution and cooling rate are investigated. The following parameters are focused:

(1) Intracellular water retention ratio Y_w, defined as the mass ratio of residual water to dry mass; (2) Supercooling degree of intracellular solution ΔT_{si}; (3) Mass fraction of intracellular electrolytes W_e^{in}; (4) Critical cooling rate B_{cr}, defined as the cooling rate beyond which intracellular ice nucleation will happen.

3 Results and Discussion

3.1 Selection of Supercooling Degree of Extracellular Solution ΔT_{se} and E_{aL} at Subzero Temperature

The supercooling degree of extracellular solution ΔT_{se} at the moment of ice nucleation depends on many factors including surface condition of the solution container. Usually it is a random value within a range, whereas it is set at fixed value here for simplification. Figs. 1a and 1b show the effects of ΔT_{se} on Y_w and supercooling degree of intracellular solution ΔT_{si}. The calculation is done with the initial conditions as follows: Total mass fraction of extracellular solutes $W_{tot}^0 = 10$ wt%; Mass ratio of nonelectrolyte to electrolyte $R_1^{'} = 15$; Mass ratio of trehalose to bovine serum albumin $R_2^{'} = 1$. It can be noted the impact of ΔT_{se} at medium cooling rate is obvious. Considering the glass vial and the filling volume (1–2 ml) used in our previous experiments, $\Delta T_{se} = 5$ K is adopted according to the average of experimental measurements. It is used for all the following calculations.

Subzero temperature may cause phase transition of cell membrane, leading to mechanism change of water transport and increase of ð,ðí [32]. For human platelets, there is little reported data about this, therefore, four values are tested to watch their impacts on Y_w and B_{cr}. While E_{aL} = 62.787, 75.344, 94.181, 125.574 kJ/mol (i.e., 1×, 1.2×, 1.5×, 2× E_{aL} at above zero degree), the change Y_w of with temperature is shown in Fig. 2 at two kinds of cooling velocity, 1 K/min and 50 K/min. On the other hand, the corresponding critical cooling rate B_{cr} = 97, 45, 26, 15 K/min. Our previous experiments illustrated that the optimum cooling rate was about 20 K/min under calculated case [33]. B_{cr} Should be a little larger than the optimum cooling rate so that intracellular ice formation (IIF) is totally avoided. Thus, E_{aL} = 75.344 kJ/mol and B = 10 K/min are adopted in the following analysis about the impacts of lyoprotectant.

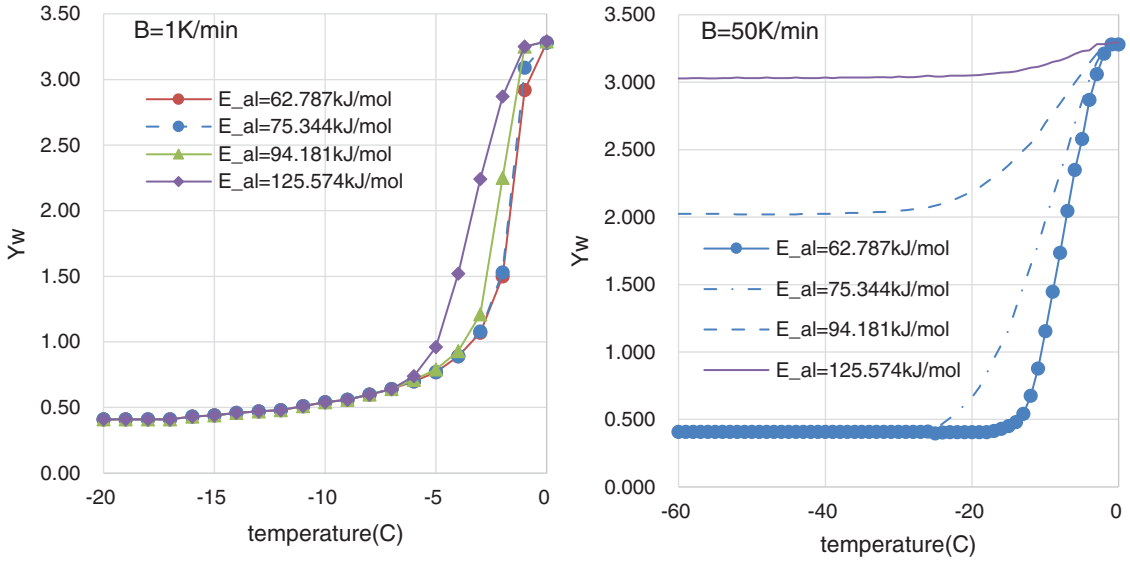

(a) (b)

Figure 2: Sensitivity analysis on activation energy of hydraulic conductivity E_{aL} (a) Y_w *vs.* temperature at B = 1 K/min, (b) Y_w *vs.* temperature at B = 50 K/min

3.2 Effects of Protectants

The protectants are necessary for successful lyophilization of cells. They can be categorized into two groups: those that can penetrate cell membrane (glycerol, ME_2SO) and those that cannot penetrate cell membrane (saccharides, proteins). In most practices or researches of freeze-drying of cells, impermeable protectants are used. Permeable protectants may exert positive influences during the freezing stage, so they were considered in some researches [19,34]. Loading trehalose into cells have been proved to be beneficial and realized through various ways [35]. Here the loading quantity of trehalose and the inclusion of permeable protectant will be studied of their effects on intracellular water retention ratio Y_w and supercooling degree of intracellular solution ΔT_{si}.

Figs. 3a and 3b show the calculation results for various W_{tot}^0 when $R_1^{'} = 15$, $R_2^{'} = 1$, B = 10 K/min. As W_{tot}^0 increases from 5 wt% to 20 wt%, the final Y_w does not change, but the intracellular solution will undergo much higher supercooling degree. Both BSA and trehalose acts as extracellular protectant, the effects of changing their fraction ratio, $R_2^{'}$, can be demonstrated in Figs. 4a and 4b ($R_1^{'} = 15$, $W_{tot}^0 = 10wt\%$, B = 10 K/min). With increasing $R_2^{'}$ or trehalose fraction, Y_w and ΔT_{si} tends to be smaller during the cooling, but the final Y_w remains unchanged.

The effects of loading trehalose can be viewed from Figs. 5a and 5b. When the molal concentration of intracellular trehalose, m_{Tre}^{in} , increases from 0 to 0.05 mol/kg, the final Y_w decreases from 0.4101 to 0.4042. The loading trehalose will increase the dry mass in the cell. While 0.05 mol/kg trehalose is loaded, the total quantity of residual water at the end of freezing may raise by 4.93%. On the whole, the effects of loading trehalose on Y_w and ΔT_{si} are small. In fact, if intracellular solution is regarded as quaternary solution containing NaCl, trehalose and BSA, their thermophysical property changes are very limited after the loading of 0.05 mol/kg trehalose [36].

Figs. 6a and 6b display the effects of volume fraction of permeable lyoprotectant Me_2SO, c_0^{ME}, on Y_w and ΔT_{si}. The calculation is done under the following conditions: $W_{tot}^0 = 10wt\%$, $R_1^{'} = 15$, $R_2^{'} = 1$, B = 10 K/min. The addition of Me_2SO can lower the concentration of electrolytes after freezing and alleviate relevant injury to the cell. From Fig. 5, it can be noted that the final Y_w increases after the addition.

While c_0^{ME} changes from 0% to 5% v/v, the final Y_w increases from 0.41 to 0.56, nearly by 40%. The addition of Me_2SO also leads to the changes of composition of intracellular and extracellular solutions after freezing concentration. The glass transition temperatures of both solutions will be decreased, thus lower product temperature has to be kept during the drying process, and the drying time will be prolonged.

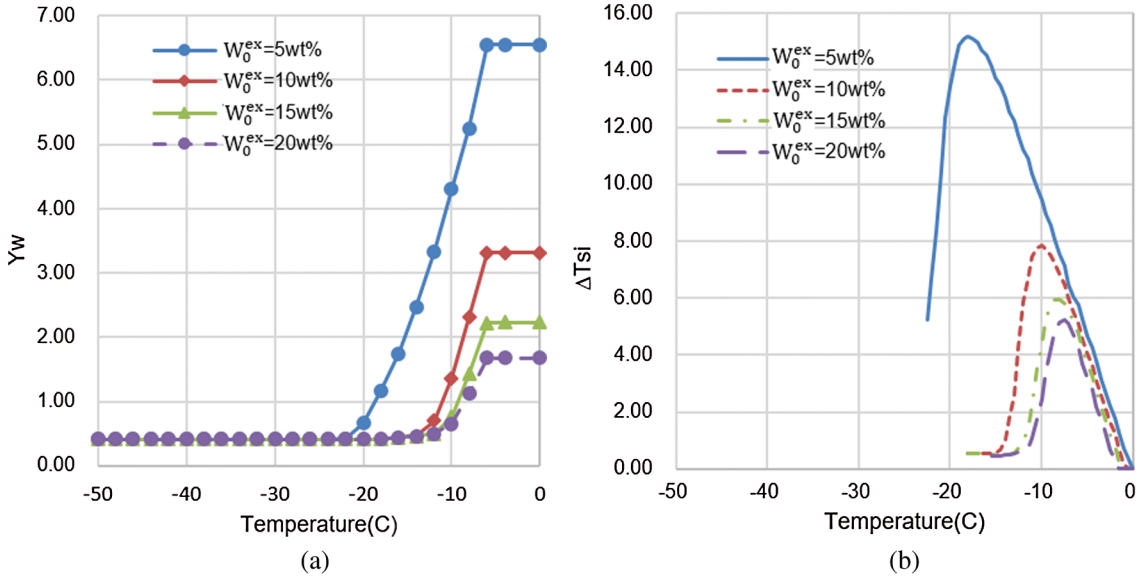

Figure 3: The effects of mass fraction of extracellular nonpermeable lyoprotectants W_0^{ex} on intracellular water retention ratio Y_w and supercooling degree of intracellular solution ΔT_{si}. (a) Y_w *vs.* temperature at different W_0^{ex}, (b) ΔT_{si} *vs.* temperature at different W_0^{ex}

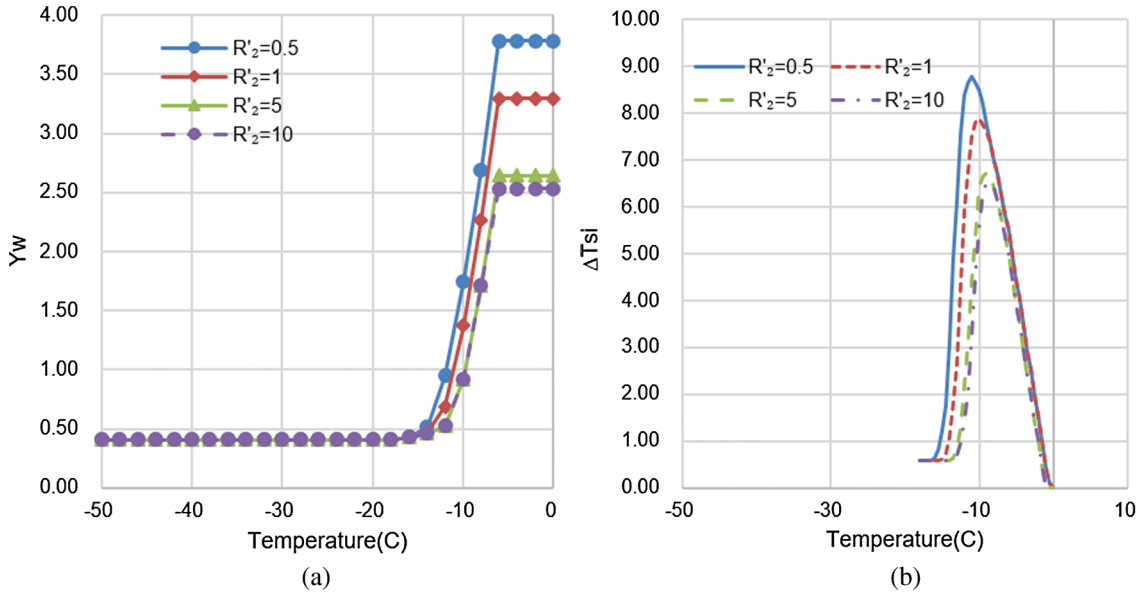

Figure 4: The effects of mass fraction ratio of extracellular trehalose to bovine serum albumin $R_2^{'}$ on intracellular water retention ratio Y_w and supercooling degree of intracellular solution ΔT_{si}. (a) Y_w *vs.* temperature at different $R_2^{'}$, (b) ΔT_{si} *vs.* temperature at different $R_2^{'}$

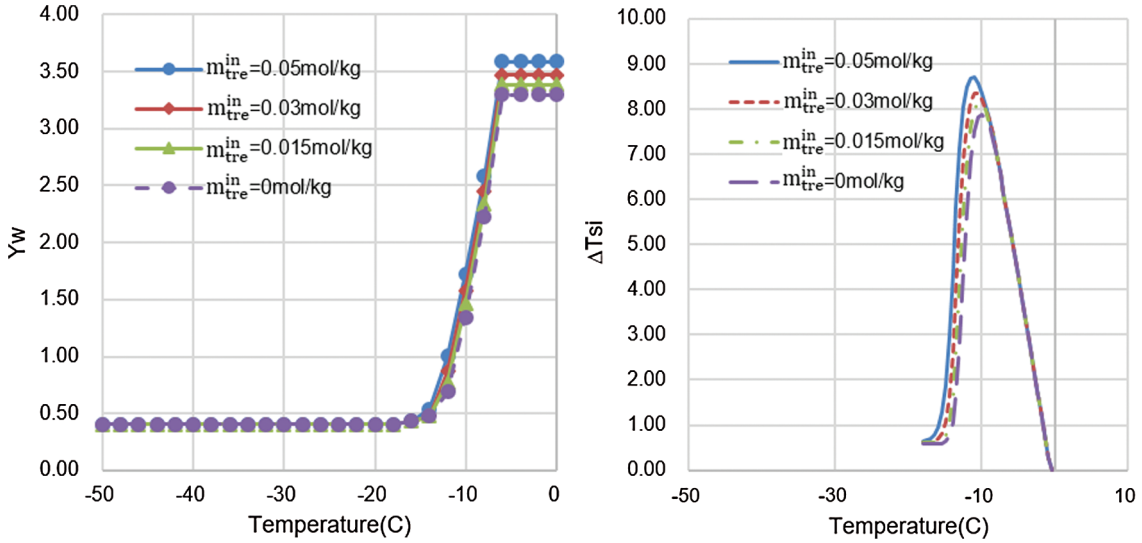

Figure 5: The effects of mole concentration of intracellular loaded trehalose m^{in}_{tre} on intracellular water retention ratio Y_w and supercooling degree of intracellular solution ΔT_{si}. (a) Y_w *vs.* temperature at different m^{in}_{tre}, (b) ΔT_{si} *vs.* temperature at different m^{in}_{tre}

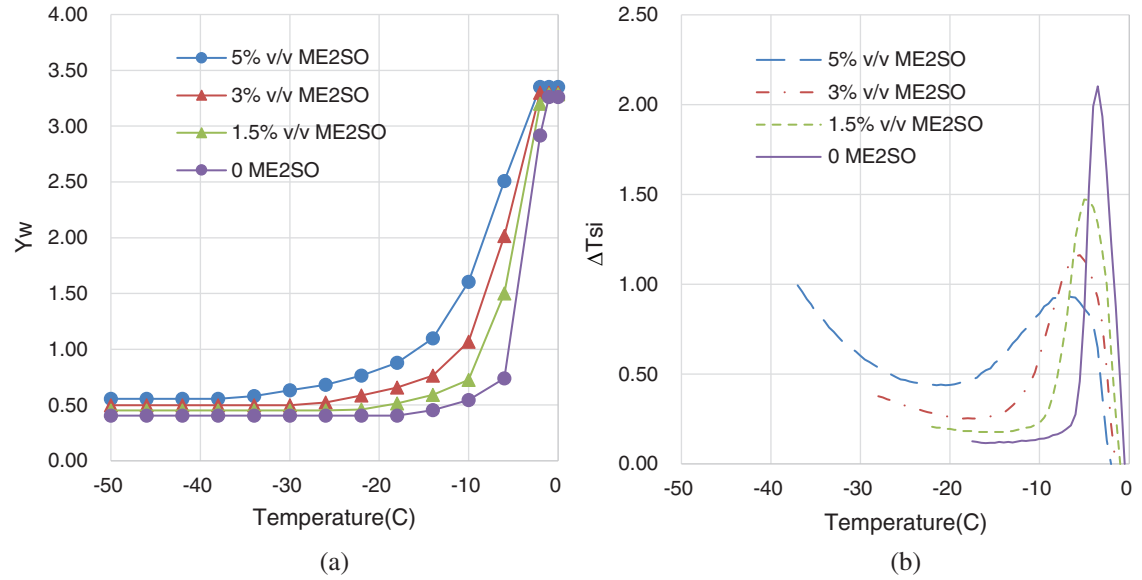

Figure 6: The effects of volume fraction of permeable lyoprotectant Me_2SO c_0^{ME} on intracellular water retention ratio Y_w and supercooling degree of intracellular solution ΔT_{si}. (a) Y_w *vs.* temperature at different c_0^{ME}, (b) ΔT_{si} *vs.* temperature at different c_0^{ME}

3.3 Discussion

Computer modeling is a powerful tool in engineering, providing the opportunity for us to change different parameters easily and cheaply to study their effects, as demonstrated by numerical investigations for behavior characteristics of metals under impact loading by Hedayati et al. [37,38]. For cases which

are difficult to carry out experiments or measurements, numerical modelling will be of great help [39,40]. In the field of cell preservation, there have been many modeling approaches for cell freezing, which appeared mostly in cryopreservation and focused on IIF and ice crystal growth such as those in the literatures [41,42]. The present study pays more attentions to IAC in freezing stage of a lyophilization process, so more elaborate assumptions are made for the intracellular composition. The intracellular and extracellular solutions are treated as non-ideal solutions, using a multi-solute osmotic Virial equation to calculate the osmolality. Experimental results on osmolality can effectively increase the accuracy of the equation. Similar treatments could be found in the literatures. Freitas et al. [43] made a simulation of permeation process in islet issue, assuming that intracellular solution was composed of electrolyte, small organic molecule and protein. Ross-Rodriguez et al. [44] presumed the intracellular solution of hematopoietic stem cell as quaternary solution composing of sodium chloride, potassium chloride, protein and water, and specified the thermodynamic property of protein as that of hemoglobin. IIF is also considered in our model. The cooling velocity is chosen according to practice, ensuring avoidance of IIF, but maybe not the optimum which is determined satisfying the requirement of cryopreservation. Sensitivity analyses are done with activation energy of hydraulic conductivity E_{aL} and supercooling degree of extracellular solution ΔT_{se}. As the solution volume, the container type and the cooling method change, ΔT_{se} may vary from a few degrees to more than ten degrees. If active seeding is adopted, a fixed ΔT_{se} can be realized. The effect of ΔT_{se} on IAC needs to be paid attention.

As demonstrated by the simulation, although the protectants presenting inside and outside the cell have impacts on the final Y_w at the end of freezing, the influence levels for different aspects are varying. Permeable protectant Me_2SO has multiple effects. It can provide protection during the freezing stage, but it increases the final Y_w significantly and decreases the admissible drying temperature. The comprehensive effects will be substantially increased drying time. A small fraction of may be preferable should it be used as protectant. Loading trehalose into cell at a concentration of 0.05 mol/kg decreases Y_w slightly, but the total water retention in the cell increases by nearly 5%, a medium level that needs attention. The effects of extracellular protectants on the final Y_w are small within the ranges investigated ($W_{tot}^0 = 5 \sim 20$wt%, $R_2^{'} = 0.5 \sim 10$). Although these results are obtained when ΔT_{se} is set at 5 K, for ΔT_{se} other than 5 K, the trends of these effects will not change. These qualitative and quantitative analyses on cell water retention create a new angle for lyoprotectant design.

4 Conclusion

Freeze-dried human platelets can be stored at room temperature for months. Low moisture content is the key index for the product. When cells are freeze-dried, there are differences between micro intra and extra domains. Due to the membrane resistance of water transport, IAC is higher than extracellular water content in freeze-dried product. This study investigates the effects of several factors on IAC after freezing by simulation. It is found that trehalose loading and Me_2SO inclusion will increase the water retention at the end of freezing, most of which has to be removed during the drying stage. These theoretical results will offer guidance for better design of freeze-drying protocol.

Funding Statement: This work was supported by the National Natural Science Foundation of China [Grant No. 51876185] and archaeological artifact protection technology project of Zhejiang Province Grant No. 2017008].

Conflicts of Interest: The authors declare that they have no conflicts of interest to report regarding the present study.

References

1. Willem, F. W., Harriëtte, O. (2015). *Cryopreservation and freeze-drying protocols*. New York, USA: Springer Science+Business Media.

2. Kanias, T., Acker, J. P. (2006). Mammalian cell desiccation: Facing the challenges. *Cell Preservation Technology, 4(4),* 253–277. DOI 10.1089/cpt.2006.9996.
3. Zhang, M., Oldenhof, H., Sydykov, B., Bigalk, J., Sieme, H. et al. (2017). Freeze-drying of mammalian cells using trehalose: Preservation of DNA integrity. *Scientific Reports, 7(1),* 1–10. DOI 10.1038/s41598-016-0028-x.
4. Wolkers, W. F., Walker, N. J., Tamari, Y., Tablin, F., Crowe, J. H. (2003). Towards a clinical application of freeze-dried human platelets. *Cell Preservation Technology, 1(3),* 175–188. DOI 10.1089/153834402765035617.
5. Wang, J. X., Yang, C., Wang, W., Liu, M. X., Ren, S. P. et al. (2011). Stability of lyophilized human platelets loaded with small molecule carbohydrates. *Cryo-Letters, 32(2),* 123–130.
6. Han, Y., Quan, G. B., Liu, X. Z., Ma, E. P., Liu, A. et al. (2005). Improved preservation of human red blood cells by lyophilization. *Cryobiology, 51(2),* 152–164. DOI 10.1016/j.cryobiol.2005.06.002.
7. Arav, A., Natan, D. (2012). Freeze drying of red blood cells: The use of directional freezing and a new radio frequency lyophilization device. *Biopreservation and Biobanking, 10(4),* 386–394. DOI 10.1089/bio.2012.0021.
8. Martins, C. F., Báo, S. N., Dode, M. N., Correa, G. A., Rumpf, R. (2007). Effects of freeze-drying on cytology, ultrastructure, DNA fragmentation, and fertilizing ability of bovine sperm. *Theriogenology, 67(8),* 1307–1315. DOI 10.1016/j.theriogenology.2007.01.015.
9. Said, S., Afiati, F., Maulana, T. (2015). Study on changes of sperm head morphometry and DNA integrity of freeze-dried bovine spermatozoa. *Journal of the Indonesian Tropical Animal Agriculture, 40(3),* 145–152. DOI 10.14710/jitaa.40.3.145-152.
10. Zhou, J., Zhang, C., Liu, J., Fan, L., Yang, L. (2011). Loading solution prevents activation damage of human platelets before lyophilization. *Cryobiology, 63(3),* 229–234. DOI 10.1016/j.cryobiol.2011.08.007.
11. Fan, J. L., Xu, X. G., Zhang, S. Z., Xu, M. J., Zhu, F. M. et al. (2011). Optimization study on the rehydration process of lyophilized human platelets. *Chinese Science Bulletin, 56(4),* 455–460. DOI 10.1007/s11434-011-4381-7.
12. Soejima, K., Shimoda, K., Kashimura, T., Yamaki, T., Kono, T. et al. (2013). Wound dressing material containing lyophilized allogeneic cultured cells. *Cryobiology, 66(3),* 210–214. DOI 10.1016/j.cryobiol.2013.02.001.
13. Sekhon, U. D. S., Sen, G. A. (2018). Platelets and platelet-inspired biomaterials technologies in wound healing applications. *ACS Biomaterials Science & Engineering, 4(4),* 1176–1192. DOI 10.1021/acsbiomaterials.7b00013.
14. Nakagawa, K., Ochiai, T. (2015). A mathematical model of multi-dimensional freeze-drying for food products. *Journal of Food Engineering, 161,* 55–67. DOI 10.1016/j.jfoodeng.2015.03.033.
15. Rasetto, V., Marchisio, D. L., Fissore, D., Barresi, A. A. (2010). On the use of a dual-scale model to improve understanding of a pharmaceutical freeze-drying process. *Journal of Pharmaceutical Sciences, 99(10),* 4337–4350. DOI 10.1002/jps.22127.
16. Benson, J. D., Kearsley, A. J., Higgins, A. Z. (2012). Mathematical optimization of procedures for cryoprotectant equilibration using a toxicity cost function. *Cryobiology, 64(3),* 144–151. DOI 10.1016/j.cryobiol.2012.01.001.
17. Cui, Z. F., Dykhuizen, R. C., Nerem, R. M., Sembanis, A. (2002). Modeling of cryopreservation of engineered tissues with one-dimensional geometry. *Biotechnology Progress, 18(2),* 354–361. DOI 10.1021/bp0101886.
18. Zhao, G., He, L., Zhang, H., Ding, W., Liu, Z. et al. (2004). Trapped water of human erythrocytes and its application in cryopreservation. *Biophysical Chemistry, 107(2),* 189–195. DOI 10.1016/S0301-4622(03)00211-4.
19. Han, Y., Quan, G. B., Liu, X. Z., Ma, E. P., Liu, A. et al. (2005). Improved preservation of human red blood cells by lyophilization. *Cryobiology, 51(2),* 152–164. DOI 10.1016/j.cryobiol.2005.06.002.
20. Mazur, P. (1963). Kinetics of water loss from cells at subzero temperatures and the likelihood of intracellular freezing. *Journal of General Physiology, 47(2),* 347–369. DOI 10.1085/jgp.47.2.347.
21. Amitage, W. J. (1986). Effect of solute concentration on intracellular water volume and hydraulic conductivity of human blood platelets. *Journal of Physiology, 374(1),* 375–385. DOI 10.1113/jphysiol.1986.sp016085.
22. Levin, R. L., Cravalho, E. G., Huggins, C. E. (1976). Effect of hydration on the water content of human erythrocytes. *Biophysical Journal, 16(12),* 1411–1426. DOI 10.1016/S0006-3495(76)85784-0.
23. Buitink, J., Leprince, O. (2004). Glass formation in plant anhydrobiotes: Survival in the dry state. *Cryobiology, 48 (3),* 215–228. DOI 10.1016/j.cryobiol.2004.02.011.

24. Prickett, R. C., Elliott, J. A., McGann, L. E. (2011). Application of the multisolute osmotic virial equation to solutions containing electrolytes. *Journal of Physical Chemistry B, 115(49),* 14531–14543. DOI 10.1021/jp206011m.
25. Xu, M. J. (2015). *Theoretical and experimental study on the freezing and pre-hydration process of platelets lyophilization*. Hangzhou, China: Zhejiang University Press.
26. Corti, H. R., Angell, C. A., Auffret, T., Levine, H., Buera, M. P. et al. (2010). Empirical and theoretical models of equilibrium and non-equilibrium transition temperatures of supplemented phase diagrams in aqueous systems (IUPAC Technical Report). *Pure and Applied Chemistry, 82(5),* 1065–1098. DOI 10.1351/PAC-REP-09-10-24.
27. Elmoazzen, H. Y., Elliott, J. A. W., McGann, L. E. (2009). Osmotic transport across cell membranes in nondilute solutions: A new nondilute solute transport equation. *Biophysical Journal, 96(7),* 2559–2571. DOI 10.1016/j.bpj.2008.12.3929.
28. Woods, E. J., Liu, J., Gilmore, J. A., Reid, T. J., Gao, D. Y. et al. (1999). Determination of human platelet membrane permeability coefficients using the Kedem-katchalsky formalism: Estimates from two- *vs.* three-parameter fits. *Cryobiology, 38(3),* 200–208. DOI 10.1006/cryo.1998.2146.
29. Liu, J. H., Ouyang, X. L., Lü, C. L., Gao, D. (2002). Thermometry of intracellular ice crystal formation in cryopreserved platelets. *Chinese Journal of Experimental Hematology, 10(6),* 574–576.
30. Pitt, R. E., Steponkus, P. L. (1989). Quantitative analysis of the probability of intracellular ice formation during freezing of isolated protoplasts. *Cryobiology, 26(1),* 44–63. DOI 10.1016/0011-2240(89)90032-1.
31. Xu, M., Chen, G., Zhang, C., Zhang, S. (2017). Study on the unfrozen water quantity of maximally freeze-concentrated solutions for multicomponent lyoprotectants. *Journal of Pharmaceutical Sciences, 106(1),* 83–91. DOI 10.1016/j.xphs.2016.05.007.
32. Akhoondi, M., Oldenhof, H., Stoll, C., Sieme, H., Wolkers, W. F. (2011). Membrane hydraulic permeability changes during cooling of mammalian cells. *Biochimica et Biophysica Acta (BBA)—Biomembranes, 1808(3),* 642–648. DOI 10.1016/j.bbamem.2010.11.021.
33. Fan, J. L. (2009). *Study on the optimization of freeze-drying protocol for human platelets*. Hangzhou, China: Zhejiang University Press.
34. Gao, D. Y., Neff, K., Xiao, H. Y., Matsubayashi, H., Cui, X. D. P. et al. (1999). Development of optimal techniques for cryopreservation of human platelets: I. Platelet activation during cold storage (at 22 and 8°C) and cryopreservation. *Cryobiology, 38(3),* 225–235. DOI 10.1006/cryo.1999.2162.
35. Stewart, S., He, X. (2019). Intracellular delivery of trehalose for cell banking. *Langmuir: ACS Journal of Surfaces and Colloids, 35(23),* 7414–7422. DOI 10.1021/acs.langmuir.8b02015.
36. Lynch, A. L., Slater, N. K. H. (2011). Influence of intracellular trehalose concentration and pre-freeze cell volume on the cryosurvival of rapidly frozen human erythrocytes. *Cryobiology, 63(1),* 26–31. DOI 10.1016/j.cryobiol.2011.04.005.
37. Hedayati, E., Vahedi, M. (2017). Numerical investigation of penetration in ceramic/aluminum targets using smoothed particle hydrodynamics method and presenting a modified analytical model. *Computer Modeling in Engineering & Sciences, 113(3),* 295–323.
38. Hedayati, E., Vahedi, M. (2018). Evaluating impact resistance of aluminum 6061-t651 plate using smoothed particle hydrodynamics method. *Defence Science Journal, 68(3),* 251–259. DOI 10.14429/dsj.68.11635.
39. Suri, Y., Sheikh, Z. I., Hossain, M. (2020). Numerical modelling of proppant transport in hydraulic fractures. *Fluid Dynamics & Materials Processing, 16(2),* 297–337. DOI 10.32604/fdmp.2020.08421.
40. Xu, T. Y., Zhang, L. X. (2020). Analysis of water transport inside a plant xylem vessel with pitted thickening. *Fluid Dynamics & Materials Processing, 16(3),* 525–536. DOI 10.32604/fdmp.2020.09618.
41. Zhao, G., Xu, Y., Ding, W., Hu, M. (2013). Numerical simulation of water transport and intracellular ice formation for freezing of endothelial cells. *Cryo-Letters, 34(1),* 40–51.
42. De Freitas, R. C., Diller, K. R. (2004). Intracellular ice formation in three-dimensional tissues: Pancreatic islets. *Cell Preservation Technology, 2(1),* 19–28. DOI 10.1089/153834404322708727.

43. De Freitas, R. C., Diller, K. R., Lachenbruch, C. A., Merchant, F. A. (1998). Network thermodynamic model of coupled transport in a multicellular tissue—The islet of Langerhans. *Annals of the New York Academy of Sciences, 858,* 191–204. DOI 10.1111/j.1749-6632.1998.tb10153.x.

44. Ross-Rodriguez, L. U., Elliott, J. A., McGann, L. E. (2012). Non-ideal solution thermodynamics of cytoplasm. *Biopreservation and Biobanking, 10(5),* 462–471. DOI 10.1089/bio.2012.0027.